AGU PUBLICATIONS

Geophysical Research Letters

RESEARCH LETTER
10.1002/2014GL062411

**Key Points:**
- First 3-D meteor simulations
- Shows meteor instabilities and turbulence
- Allows better understanding of meteor evolution

**Supporting Information:**
- Readme
- Movie S1
- Movie S2

**Correspondence to:**
M. M. Oppenheim,
meerso@bu.edu

**Citation:**
Oppenheim, M. M., and Y. S. Dimant (2015), First 3-D simulations of meteor plasma dynamics and turbulence, *Geophys. Res. Lett.*, *42*, 681–687, doi:10.1002/2014GL062411.

Received 5 NOV 2014
Accepted 8 JAN 2015
Accepted article online 11 JAN 2015
Published online 9 FEB 2015

# First 3-D simulations of meteor plasma dynamics and turbulence

**Meers M. Oppenheim[1] and Yakov S. Dimant[1]**

[1]Center for Space Physics, Boston University, Boston, Massachusetts, USA

**Abstract** Millions of small but detectable meteors hit the Earth's atmosphere every second, creating trails of hot plasma that turbulently diffuse into the background atmosphere. For over 60 years, radars have detected meteor plasmas and used these signals to infer characteristics of the meteoroid population and upper atmosphere, but, despite the importance of meteor radar measurements, the complex processes by which these plasmas evolve have never been thoroughly explained or modeled. In this paper, we present the first fully 3-D simulations of meteor evolution, showing meteor plasmas developing instabilities, becoming turbulent, and inhomogeneously diffusing into the background ionosphere. These instabilities explain the characteristics and strength of many radar observations, in particular the high-resolution nonspecular echoes made by large radars. The simulations reveal how meteors create strong electric fields that dig out deep plasma channels along the Earth's magnetic fields. They also allow researchers to explore the impacts of the intense winds and wind shears, commonly found at these altitudes, on meteor plasma evolution. This study will allow the development of more sophisticated models of meteor radar signals, enabling the extraction of detailed information about the properties of meteoroid particles and the atmosphere.

## 1. Introduction and Background

While an impact as large as the 2013 Chelyabinsk meteor occurs only about once a century, millions of small but detectable meteors hit the Earth's atmosphere every second. These small particles generally disintegrate as they enter the Earth's upper atmosphere creating columns of dense plasmas along their paths. Through this ablation process they produce one of the most common—but least understood—natural plasmas in the terrestrial environment. This paper presents the first fully kinetic, 3-D, simulations of the evolution of a meteor plasma from the stage where the meteor has thermalized with the neutral atmosphere until it develops into a fully turbulent diffusive plasma.

Meteor observations and meteoric materials play an important role in upper atmosphere physics. The material deposited by these small meteoric particles affects ionosphere conductivities, creates metal layers, and coalesces into dust that initiates noctilucent cloud formation and influences weather throughout the atmosphere [*McNeil et al.*, 2001; *Klekociuk et al.*, 2005; *Lebedinets et al.*, 1973]. Meteor radars have been used for decades to monitor winds between about 75 and 110 km altitude, providing data essential to upper atmosphere wind and tide modeling. Despite the importance of meteor radar measurements, the complex processes by which these plasmas evolve have never been thoroughly explained or modeled, limiting researchers' abilities to accurately interpret the measurements.

Meteoroids weighing only a few micrograms to milligrams but moving at typical speeds of between 20 and 70 km/s frequently create radar traces similar to the one shown in Figure 1. This letter addresses the question of what enables a radar to see what we call a nonspecular or range-spread meteor trail. It presents a set of simulations that explains the origin of these radar observations and shows the complex processes that occur when a meteor creates a dense plasma column that interacts with the Earth's *E* region ionosphere and the lower thermosphere.

A meteoroid entering the Earth's atmosphere will leave behind a plasma column that will expand rapidly until slowed and cooled by collisions with the much denser neutral gas of the atmosphere. The radius of the column at the time when it transitions from a rapid ballistic expansion to a slower diffusive expansion is called the initial radius of the trail and is of the order of the mean-free-path length [*Baggaley*, 1981; *Bronshten*, 1983; *Jones*, 1995]. After the column reaches this initial radius, the column of charged particles

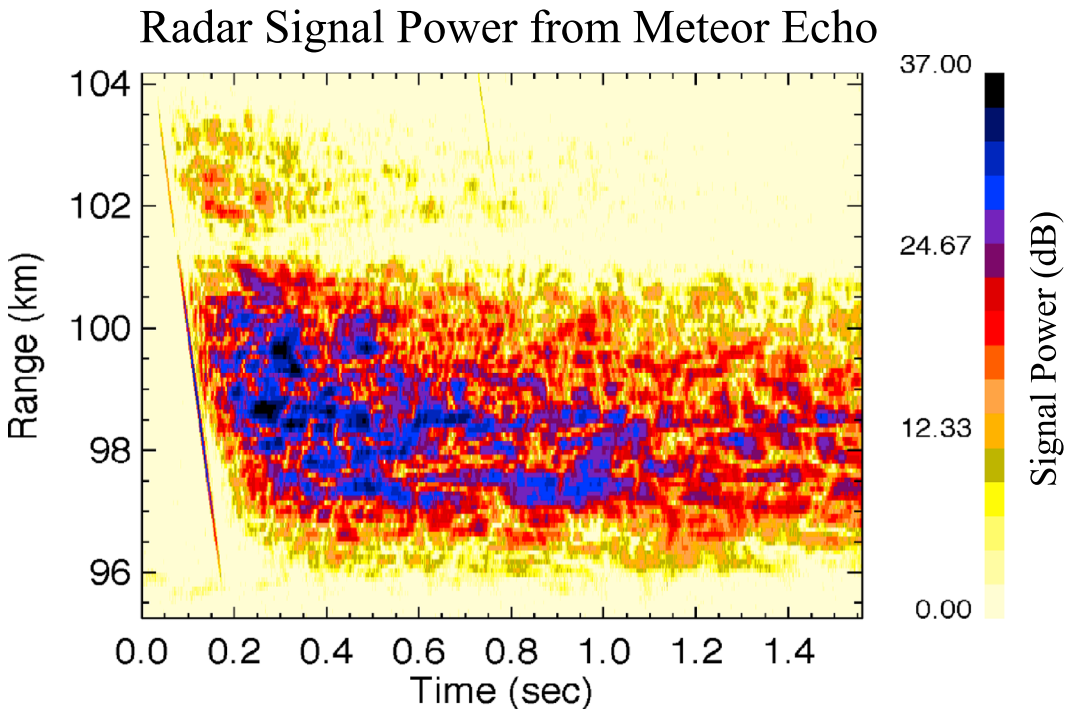


**Figure 1.** Radar power return plotted against altitude and time for a strong but not unusual meteor echo from the 50 MHz main antenna array at the Jicamarca Radio Observatory. The colors indicate the strength of the return in a log (dB) scale. The meteor head echo is the colored line on the left, and the nonspecular trail echo is the signal that extends over both range and time. The nonspecular echo only becomes visible tens of milliseconds after the head echo signal disappears. The weak signal above 101.5 km comes from the radar sidelobe, and the gap at 101.5 km occurs because the meteor passed through a radar sensitivity null.

begins diffusing outward under the influence of the geomagnetic field and often develops waves and turbulence. Eventually, after seconds to minutes, it merges with the background ionosphere.

Meteor physics has been studied episodically by astronomers, radio scientists, and physicists as new tools and needs have developed. A number of books and articles review the fundamental behavior of meteor trails and collisionally dominated plasmas [*Öpik*, 1958; *Ceplecha et al.*, 1998; *Hawkes et al.*, 2004; *Kelley*, 2009]. A number of authors have evaluated the diffusion and drift dynamics of meteor trails embedded in the collisional lower thermosphere [*Pickering and Windle*, 1970; *Jones*, 1991; *Dimant and Oppenheim*, 2006a, 2006b]. More recently, researchers have extended these studies in order to evaluate the dynamics of meteor trails subject to externally imposed electric fields [*Dimant et al.*, 2009].

The only previous kinetic simulations of meteor trail plasma evolution were limited to 2-D [*Oppenheim et al.*, 2000, 2003]. These could only reasonably model the physics of meteors with trajectories that parallel the geomagnetic field to within a few degrees, an infrequent alignment. When trying to simulate meteors aligned perpendicular to the geomagnetic field $\vec{B}_0$, they actually modeled dense plasma sheets. This 2-D approach misses much of the physics of most meteor trails as they interact with a magnetic field.

## 2. Method

This paper reports on 3-D simulation studies performed using the electrostatic parallel particle-in-cell (EPPIC) code to simulate both ions and electrons as fully kinetic, collisional plasmas [*Oppenheim and Dimant*, 2004; *Oppenheim et al.*, 2008; *Oppenheim and Dimant*, 2013]. This accurately models all plasma dynamics, including thermal effects, at the cost of substantial computer time. It applies a rapid spectral technique to determine the electrostatic field, but this method requires periodic boundary conditions. To enable the large-scale and long-duration simulations presented here, EPPIC applies a novel approach to running on massively parallel computers and has run on up to 8192 processors simultaneously with tens of billions of particles and 2 billion grid cells.

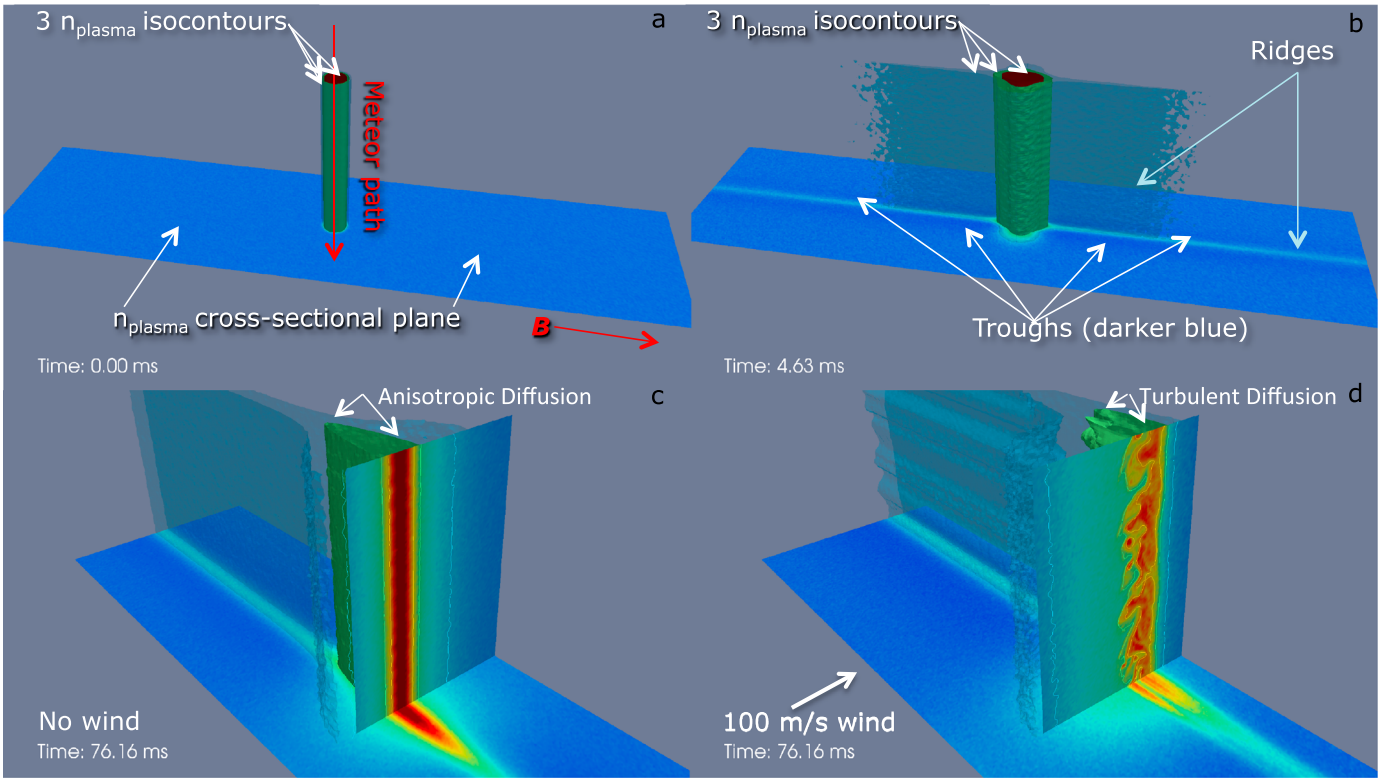


**Figure 2.** Images from two 3-D simulations of meteor evolution (best viewed at high resolution and in the dynamical animations in the supporting information Movies S1 and S2. All four images show the meteor plasma density using three isocontour surfaces parallel to the initial trail in red, green, and blue. The blue planes show a cross section of the density perpendicular to the trail. (a) The plasma distribution used to initialize the simulation with a peak density of 160 times the background density. In this case, the red, blue, and green isocontours appear as parallel tubes nestled within each other. (b) The plasma density after 4.6 ms. Here one sees the growth of the ridge and troughs connected to the meteor along $\vec{B}_0$. The ridges appear both as the translucent dark blue isocontour wings connecting to the meteor column and as light blue enhancements in the background plane. The troughs appear as the slightly darker blue plasma depletions in the background plane adjoining the ridge. Note also the distorted shape of the plasma column that develops as the meteor diffuses more rapidly along *B* than perpendicular to it. (c) The plasma density from wind-free simulation. One can see the anisotropic diffusion of the meteor and only a hint of waves. (d) The plasma density from the simulation with wind. One can see the anisotropic diffusion of the meteor and the fully developed turbulent waves. The wave structure permeates the windward side of the dense plasma column and penetrates into the meteor wings.

For numerical efficiency, fully kinetic simulations often require the modification of fundamental plasma parameters, such as the electron to ion mass ratio. However, obtaining results that accurately represent the essential physics requires that we remain within strict limitations as discussed in *Oppenheim and Dimant* [2004]. For the runs discussed here, the simulated electron mass was raised by a factor of 44 over $m_e$ as explained in *Oppenheim and Dimant* [2013].

EPPIC implements charged-neutral collisions with a hard sphere elastic collision model, where the likelihood of collision is linearly proportional to the macroparticle's velocity relative to a neutral particle (i.e., constant cross section). This technique yields average Hall and Pedersen drift rates and particle heating and cooling rates predicted by laminar fluid theory. We modify the mass of the neutral particle and the collision rate to mimic inelastic electron-neutral collision processes as described in *Oppenheim and Dimant* [2004] and *Oppenheim and Dimant* [2013]. These collisions provide the only damping or dissipation in this system except for the kinetic Landau damping.

This simulation uses periodic boundary conditions. This means that the simulated meteor plasma is infinitely long and that a periodic grid of identical meteors exists in the plane perpendicular to the column. This will necessarily impact the dynamics in a number of ways. First, the meteor is effectively infinite in length and has no start or end. Since real meteors are kilometers long and only a few meters wide at their onset, this may not create overly unphysical results. Second, neighboring meteors will influence each other, though this should only have a major impact along $\vec{B}_0$, since electrons can travel rapidly and $\vec{E}_\perp$ fields change over

long distances in this direction. In the direction perpendicular to both the trail and $\vec{B}_0$, little communication of particles or fields develops.

## 3. Results

Using some of the world's largest supercomputers, we simulate the fundamental physics of meteor evolution. This enables us to study the diffusion of the trails, their effects on the background plasma, and the development of the waves and turbulence responsible for nonspecular echoes (see Figure 1). It also allows us to explore the dependence of meteor evolution on altitude, winds, and peak meteor plasma density.

The first simulation examines meteor diffusion in a homogeneous ionosphere/thermosphere devoid of a background wind or electric field. It assumes that a meteoroid has already passed through this volume of space, leaving behind a smooth column of plasma which has expanded to the initial radius and thermalized. Therefore, this simulation begins with a background plasma plus a vertical column with a peak density 160 times the background density of 400 $cm^{-3}$ as shown in Figure 2a. We chose this peak density because it exceeds the threshold for instabilities as predicted by *Dimant and Oppenheim* [2006a] and *Dimant et al.* [2009], but since the computational cost of a simulation scales linearly with the peak density, we could not use a substantially higher value. The starting meteor plasma column density falls off as a Gaussian with a variance of 0.8 m.

All background plasma parameters were chosen to match those of *Oppenheim and Dimant* [2013], since this parameter set has been extensively tested. As in those 2013 simulations, we used a background plasma density of 400 $cm^{-3}$, a low but still reasonable value, since a lower background density leads to a higher instability growth rate. The simulation background and neutral parameters approximate the ionosphere at high latitudes at 106 km altitude. At this altitude, the ion-neutral collision rate was 315 $s^{-1}$. In the ionosphere the electron-neutral collision rate is typically 11 times the ion value but has to be reduced in the simulation because of the artificial electron to ion mass ratio. The neutral temperature is fixed at 300 K. This yields a nominal ion-neutral mean-free-path of 0.9 m.

The geomagnetic field $\vec{B}_0$ of 0.5 G is aligned along the longest axis and perpendicular to the plasma column. Changing the direction of $\vec{B}_0$ with respect to the trail makes only a small difference unless the trail and the field are aligned to within about 6°. *Dimant and Oppenheim* [2006a, 2006b] and *Dimant et al.* [2009] evaluated changes in field and drifts as a function of this angle and showed that except in the case of near-perfect alignment, they scale with the sine of the angle between the trail and $\vec{B}_0$.

The second simulation adds a neutral wind of 100 m/s blowing both perpendicular to the trail and $\vec{B}_0$. To stay in the frame of reference of the neutral wind, the simulation introduces an $\vec{E}_0 = 5\,\hat{x}$ mV/m along the trail direction.

Both simulations use the same parameters except for the $\vec{E}_0$ used in the wind simulation. The meteor plasma column is aligned parallel to $\hat{x}$, while the externally imposed magnetic field of $0.5 \times 10^{-4}$ T points in the $\hat{z}$ direction. The grid cells span to 0.1 m in all directions, making the total $256 \times 256 \times 1024$ cell simulation extend $25.6 \times 25.6 \times 102.4$ m. The simulation time step was a constant 2.5 μs for 30,464 iterations, making the entire run last just over 76 ms duration. These simulations each required 4.4 h of 4096 processors on the Stampede supercomputer.

The initial ambipolar electric fields formed as predicted by *Dimant and Oppenheim* [2006a, 2006b]. This strong $\vec{E}_\perp$ field propagates rapidly along $\vec{B}_0$ into the background plasma causing the formation of plasma ridges and troughs (or "wings") to grow as the field pushes ions into a channel connected to the meteor by $\vec{B}_0$ from adjoining regions as described in *Oppenheim and Dimant* [2006]. Figure 2b shows these troughs as they develop. The electrons travel to maintain quasineutrality, but because of their limited cross-field mobility and hall drift, they take a more complex route to this region. The periodicity of these simulations means we don't see the full extent of the wings. Instead, the wings of the central meteor merge into those of the neighboring identical meteors. This also changes the Hall and Pedersen drift paths taken by the electrons. We expect these changes to have a minimal impart on the meteor wave evolution in the plasma column.

Even after tens of milliseconds, the windless simulation shows only low-amplitude waves. Figure 2c presents a single snapshot of the density where one can see a hint of these waves (in the transition from dark red to

lighter red), but the animations make it clear that these waves exist (Note: Seen as dynamic content in the supporting information Movie S1.). From this one can assume that the instability growth rate only slightly exceeds the diffusion rate, preventing the waves from reaching a substantial amplitude or triggering turbulence. One can also see that in this case, the meteor expands more rapidly along $\vec{B}_0$ than perpendicular to it. This causes the meteor to develop an elliptical shape as it diffuses. It may help to zoom in in Figure 2 to see this.

Adding a wind leads to the development of strong waves as seen in Figure 2d. The waves appear both in the dense plasma column of the meteor and extend into the ridges and troughs. They start as relatively short wavelength waves and evolve into longer waves as they develop into a convective instability and turbulence (Note: See supporting information Movie S2.). These waves will make the meteor plasma visible to radars as nonspecular meteor trails since they will scatter radio waves in a broad range of directions as discussed below.

All simulations with winds develop waves and turbulence. We tested wind speeds ranging from 160 m/s to 40 m/s. The faster wind speed runs develop waves and turbulence more rapidly than the slower wind speed ones do. We quantified this growth rate for three wind speeds (40 m/s, 100 m/s , and 140 m/s) by evaluating $\langle E_x^2 \rangle$ which yielded *e*-folding growth rates (59 $s^{-1}$, 370 $s^{-1}$, and 480 $s^{-1}$). Also, the faster wind runs generate larger-amplitude turbulence.

## 4. Discussion and Conclusions

*Dimant and Oppenheim* [2006a, 2006b] and *Oppenheim and Dimant* [2006] used analytical theory and fluid simulations to evaluate fields and drifts in and around meteor plasmas. These papers also developed simple models of instability thresholds for a fully 3-D meteor. They did not include the effects of an external electric field on the instability threshold. *Dimant et al.* [2009] added the effects of such an external field but used a simplified model of the meteor plasma density to estimate Farley-Buneman instability thresholds. The simulations presented above allow us to explore these thresholds more accurately and to examine the nonlinear evolution of these systems, something never done before.

Turbulence develops in all simulations having winds. The plasma density irregularities associated with the turbulence will cause meteors to generate nonspecular (also called range-spread) meteor radar echoes. The highly structured plasma will reflect radio waves over a broad range of wavelengths in all directions with the strongest reflections occurring for waves aligned perpendicular to the geomagnetic field and wavelengths between tens of centimeters and tens of meters. Even if the dense central column of the meteor plasma lies outside the radar beam or within a null in the beam pattern, the wings of the trail that extend along $\vec{B}_0$ should prove highly reflective, enabling the reflection of some fraction of the radar energy. Spectral analyses of simulations like the ones described above should reveal more qualitative and quantitative features of the nonspecular meteor echoes.

The simulation without winds develops little to no turbulence. In this situation, one would not expect radars to detect a nonspecular trail echo but only a head echo or specular trail. However, observations that use nonspecular meteor trail echoes to track winds show that meteors in low wind conditions still generate full strength echoes, creating something of a mystery [*Oppenheim et al.*, 2009, 2014].

One possible explanation for this lack of turbulence is that the simulation can only model meteors with relatively modest density enhancements above the background. The meteors that make strong nonspecular trails almost certainly have peak densities orders of magnitude larger than the 160 times the background density modeled in this study. *Dimant et al.* [2009] showed that a threshold meteor density exists, below which one would not expect instabilities to develop. The present simulations exceed this threshold only by a small amount but also impose boundary conditions not modeled in the theory that may eliminate the instability. We expect that larger meteors, with their more intense density gradients, will rapidly develop large-amplitude, long-lived turbulence with little or no wind to drive them. With the ever-increasing power of modern supercomputers, it will soon become possible to model larger meteors embedded in a larger volume of background plasma.

Another explanation may be that real meteors span many kilometers in altitude and the background atmosphere changes dramatically within such a range. While little to no wind may exist in a few kilometer altitude range, above and below that quiet zone, winds almost always exist [*Larsen*, 2002; *Oppenheim et al.*,

2014]. Further, the plasma and neutral densities change rapidly in this region, with an ~8 km scale height. These simulations do not model meteors embedded in such an inhomogeneous medium. Nonetheless, multiple-kilometer-long dense plasma columns will develop ambipolar electric fields which will drive electron drifts along the column, communicating information from these different regions rapidly along the length of the meteor. This also provides an interesting set of questions which simulations can help address.

The primary weakness of this type of simulation arises from the periodic boundary conditions (BCs). Applying other types of BCs will enable us to explore the effects of the boundaries, but as typical in simulations, BCs will remain a limiting factor in meteor simulations for the foreseeable future. In particular, adding injection boundary conditions along two or four of the boundaries will allow researchers to understand the impact of these boundaries. This will become easier as computers become faster.

These simulations help us understand the evolution of meteor trails and the origin of nonspecular trail radar echoes. By comparing high-resolution meteor trail measurements with those predicted by simulations, we can assess whether we have properly modeled meteor plasma columns. It may prove necessary to add features such as dust content, atmospheric inhomogenities, and boundary conditions in order to accurately interpret these measurements. Additionally, these simulations can show us the nature of anomalous diffusion as a function of altitude and give us a more detailed understanding of the ridge and trough ("wing") formation that may play an important role in structuring the nighttime ionosphere [*Oppenheim and Dimant*, 2006].

Additional analyses and simulations should enable researchers to better understand the relationship between the external field, the background ionosphere/thermosphere, and the instability. In the near future, we envision that more accurate simulations of meteor evolution will become relatively easy. These simulations may include accurate injection of meteoroid plasma into the simulator instead of just starting with a plasma column as done here. They may include wind shears instead of steady winds. They may include inhomogeneities in the atmosphere and meteor plasma as expected in real meteors. The simulations presented above show the rich and fascinating dynamics that meteors, even in a simple system, generate.

**Acknowledgments**

Work was supported by National Science Foundation grants ATM-9986976, ATM-0332354, ATM-0334906, and ATM-0432565. The simulation codes and outputs have been archived at the NSF-supported TACC computational facility and are available upon request. The authors would also like to thank Yann Tambouret, Robert Putnam, Erik Brissom, and BU's SCV group for help in visualization. This work used XSEDE resources supported by NSF grant ACI-1053575. We also thank Budiardja and Vienne for their assistance with improving the EPPIC code which was made possible through the XSEDE ECSS program. The authors acknowledge TACC at University of Texas at Austin and NICS at University of Tennessee for providing excellent computational resources.

The Editor thanks William Baggaley and an anonymous reviewer for their assistance in evaluating this paper.

## References

Baggaley, W. J. (1981), Single wavelength measurements of the initial radii of radio meteor ionization columns, *Bull. Astron. Inst. Czech.*, *32*, 345–348.

Bronshten, V. A. (1983), *Physics of Meteoric Phenomena*, pp. 100–105, Reidel Company, Boston, Mass.

Ceplecha, Z., J. Borovicka, W. G. Elford, D. O. Revelle, R. L. Hawkes, V. Porubcan, and M. Simek (1998), Meteor phenomena and bodies, *Space Sci. Rev.*, *84*, 327–471.

Dimant, Y. S., and M. M. Oppenheim (2006a), Meteor trail diffusion and fields: 1. Simulations, *J. Geophys. Res.*, *111*, A12312, doi:10.1029/2006JA011797.

Dimant, Y. S., and M. M. Oppenheim (2006b), Meteor trail diffusion and fields: 2. Analytical theory, *J. Geophys. Res.*, *111*, A12313, doi:10.1029/2006JA011798.

Dimant, Y. S., M. M. Oppenheim, and G. M. Milikh (2009), Meteor plasma trails: Effects of external electric field, *Ann. Geophys.*, *27*, 279–296.

Hawkes, R., and I. Mann, and P. Brown (Eds.) (2004), *Modern Meteor Science: An Interdisciplinary View*, Springer, Dordrecht.

Jones, W. (1991), Theory of diffusion of meteor trains in the geomagnetic field, *Planet. Space Sci.*, *39*, 1283–1288.

Jones, W. (1995), Theory of the initial radius of meteor trains, *Mon. Not. R. Astron. Soc.*, *275*, 812–818.

Kelley, M. C. (2009), *The Earth's Ionosphere: Plasma Physics and Electrodynamics*, Academic Press, New York.

Klekociuk, A. R., P. G. Brown, D. W. Pack, D. O. Revelle, W. N. Edwards, R. E. Spalding, E. Tagliaferri, B. B. Yoo, and J. Zagari (2005), Meteoritic dust from the atmospheric disintegration of a large meteoroid, *Nature*, *436*, 1132–1135.

Larsen, M. F. (2002), Winds and shears in the mesosphere and lower thermosphere: Results from four decades of chemical release wind measurements, *J. Geophys. Res.*, *107*(A8), 1215, doi:10.1029/2001JA000218.

Lebedinets, V., A. Manochina, and V. Shushkova (1973), Interaction of the lower thermosphere with the solid component of the interplanetary medium, *Planet. Space Sci.*, *21*, 1317–1332.

McNeil, W. J., R. A. Dressler, and E. Murad (2001), Impact of a major meteor storm on Earth's ionosphere: A modeling study, *J. Geophys. Res.*, *106*, 10,477–10,465.

Öpik, E. J. (1958), *Physics of Meteor Flight in the Atmosphere*, Interscience Publishers, New York.

Oppenheim, M. M., and Y. S. Dimant (2004), Ion thermal effects on E-region instabilities: 2-D kinetic simulations, *J. Atmos. Sol. Terr. Phys.*, *66*, 1639–1654.

Oppenheim, M. M., and Y. Dimant (2006), Meteor induced ridge and trough formation and the structuring of the nighttime E-region ionosphere, *Geophys. Res. Lett.*, *33*, L24105, doi:10.1029/2006GL028267.

Oppenheim, M. M., and Y. S. Dimant (2013), Kinetic simulations of 3-D Farley-Buneman turbulence and anomalous electron heating, *J. Geophys. Res. Space Physics*, *118*, 1306–1318, doi:10.1002/jgra.50196.

Oppenheim, M. M., A. F. vom Endt, and L. P. Dyrud (2000), Electrodynamics of meteor trail evolution in the equatorial E-region ionosphere, *Geophys. Res. Lett.*, *27*(19), 3173–3176.

Oppenheim, M. M., L. P. Dyrud, and A. F. vom Endt (2003), Plasma instabilities in meteor trails: 2-d simulation studies, *J. Geophys. Res.*, *108*(A2), 1064, doi:10.1029/2002JA009549.

Oppenheim, M. M., Y. Dimant, and L. P. Dyrud (2008), Large-scale simulations of 2-D fully kinetic Farley-Buneman turbulence, *Ann. Geophys.*, *26*, 543–553.

Oppenheim, M. M., G. Sugar, N. O. Slowey, E. Bass, J. L. Chau, and S. Close (2009), Remote sensing lower thermosphere wind profiles using non-specular meteor echoes, *Geophys. Res. Lett.*, *36*, L09817, doi:10.1029/2009GL037353.

Oppenheim, M. M., S. Arredondo, and G. Sugar (2014), Intense winds and shears in the equatorial lower thermosphere measured by high-resolution nonspecular meteor radar, *J. Geophys. Res. Space Physics*, *119*, 2178–2186, doi:10.1002/2013JA019272.

Pickering, W. M., and D. W. Windle (1970), The diffusion of meteor trains, *Planet. Space Sci.*, *18*, 1153–1161.